

Controls for a Nonlinear System Arising in Vision Based Landing of Airliners

Laurent Burlion, Victor Gibert, Michael Malisoff, Frederic Mazenc

▶ **To cite this version:**

Laurent Burlion, Victor Gibert, Michael Malisoff, Frederic Mazenc. Controls for a Nonlinear System Arising in Vision Based Landing of Airliners. International Journal of Robust and Nonlinear Control, 2021, 10.1002/rnc.5332 . hal-03483398

HAL Id: hal-03483398

https://inria.hal.science/hal-03483398

Submitted on 16 Dec 2021

HAL is a multi-disciplinary open access archive for the deposit and dissemination of scientific research documents, whether they are published or not. The documents may come from teaching and research institutions in France or abroad, or from public or private research centers.

L'archive ouverte pluridisciplinaire **HAL**, est destinée au dépôt et à la diffusion de documents scientifiques de niveau recherche, publiés ou non, émanant des établissements d'enseignement et de recherche français ou étrangers, des laboratoires publics ou privés.

Controls for a Nonlinear System Arising in Vision Based Landing of Airliners

Laurent Burlion Victor Gibert Michael Malisoff Frederic Mazenc

Abstract

We use a novel backstepping method to solve a stabilization problem for a nonlinear system with delayed sampled outputs that are not accurately measured. We provide an application to a system arising in vision based landing of airliners that includes coupling between the lateral and longitudinal dynamics, for which we provide performance guarantees in the presence of the delay, nonlinearity, and sampling. Our major contributions are (a) designs of lateral and longitudinal control laws for our nonlinear model of an aircraft landing on an unequipped runway, (b) mathematical proofs that our controls ensure that the aircraft being modeled achieves the desired alignment with the runway during its align phase, under the sampling and delays that arise from image processing of visual information, and (c) comparative simulations exhibiting the considerable improvement in the control performance compared with previous methods that did not take the coupling of the dynamics or delayed sampled measurements into account.

I. Introduction

Backstepping is a valuable technique for finding controls and has been used in many aerospace and other applications; see for instance [1]–[3], and [4]. The papers [5] and [6] introduced a significantly different backstepping approach, which produces artificial pointwise delays in the controls, meaning, delays are present in the controls even if current state values are available for measurement. The artificial delays approach can circumvent the problem of finding Lie derivatives of the fictitious controls from classical backstepping, to relax the smoothness requirement that was placed on the fictitious controls in previous contributions on backstepping. Also, for

Key words: Delays, sampling, robustness, aerospace.

Burlion: Assistant Professor, Department of Mechanical and Aerospace Engineering, 98 Brett Road, Rutgers University, Piscataway, NJ 08854, USA, laurent.burlion (at) rutgers.edu.

Gibert: Advanced Flight Control Engineer, Airbus Operations, S.A.S, 31027 Toulouse, France, victor.gibert (at) airbus.com.

Malisoff: Distinguished Professor, Department of Mathematics, 303 Lockett Hall, Louisiana State University, Baton Rouge, LA 70803-4918, USA, malisoff (at) lsu.edu. Supported by US National Science Foundation Grant 1711299.

Mazenc: DR2, Inria EPI DISCO, L2S-CNRS-CentraleSupélec, 3 rue Joliot Curie, 91192, Gif-sur-Yvette, France, frederic.mazenc (at) l2s.centralesupelec.fr.

many systems of feedback or feedforward form, the approach from [5] and [6] can be applied to determine bounded feedbacks; see [7]–[12], and [13] for motivation for boundedness of controls.

This work adapts the approach from [5] and [6] to a control problem that is motivated by an aerospace problem that was a focus of the VISIOLAND project; see Section III. We are interested in the automatic landing of an aircraft, where because the runway is unequipped, the aircraft must rely on an embedded video camera which, from the control point of view, presents the problem of controlling a perspective dynamical system [14]. Except for [15] and [16], works on this problem were confined to linearized dynamics; see [17] and [18]. The linear systems are computed using knowledge of the runway dimensions, or, equivalently, relative altitude measurements. The work [19] did not assume that the runway was known but used a linearized longitudinal dynamics and a saturated control. However, it is well known that it is important for models to include the most important nonlinearities of a physical system, in order to provide controls that provide performance guarantees under uncertainties that commonly occur in control engineering [22].

Therefore, this work studies a nonlinear system that incorporates coupling between the lateral and longitudinal dynamics, which was not covered by previous works. The major contributions of this work are:

(a) Designs of lateral and longitudinal control laws for our nonlinear model of an aircraft landing on an unequipped runway, which we believe constitute the first time that the bounded backstepping approach from [5] and [6] has ever been applied to aircraft landing models under the delayed and uncertain measurements that prevail in aerospace applications,

(b) Mathematical proofs that the control laws ensure that the aircraft being modeled achieves the desired alignment with the runway during its align phase under the sampling and delays that arise from the required image processing of visual information, using a novel trajectory approach that overcomes the limitations of traditional linearization or Lyapunov function approaches, and

(c) Comparative simulations that exhibit the considerable improvement in the controller performance, compared with previous control methods that did not properly account for the nonlinear coupling of the dynamics or image processing that would arise in realistic aircraft applications.

We prove global asymptotic stability, using a model in Section III, which contains numerical results that apply our result; see [20] for an artificial delays approach for a complementary

landing problem without coupling. This makes it possible to provide performance guarantees that ensure global asymptotic stability under uncertain delays and sampling in the output, by incorporating known bounds from the delays and sampling into the control design. These performance guarantees were not available in the literature. This work improves on our conference version [21], which did not include proofs or measurement delays or sampling in the outputs and so could not model image processing.

We use standard notation. The standard Euclidean norm, and the induced matrix norm, are denoted by $|\cdot|$, $|\cdot|_S$ is the supremum over any set S, and $|\cdot|_\infty$ is the usual sup norm. We define Ξ_t by $\Xi_t(s) = \Xi(t+s)$ for all Ξ, $s \leq 0$, and $t \geq 0$ for which the equality is defined (which we denote by $\Phi_{i,t}$ when $\Xi = \Phi_i$ is the ith component of a vector valued function Φ). For each constant $J > 0$, let $\mathrm{sat_J}$ denote the saturation function $\mathrm{sat}_J(x) = \max\{-J, \min\{J, x\}\}$ for all $x \in \mathbb{R}$. We use the usual class of comparison functions $\mathcal{K}_\infty$ and input-to-state stability definitions [22].

II. Main Result

A. Nonlinear System

We consider the system

$$\begin{cases} \dot{q}_1 = V\big(\sin(\gamma) - \cos(\gamma)\cos(\psi)\tan(\gamma_c)\big), \quad \dot{q}_2 = V\cos(\gamma)\sin(\psi), \\ \dot{\gamma} = u_1, \quad \dot{\psi} = \frac{g}{V}\tan(\phi), \quad \dot{\phi} = u_2 \end{cases} \tag{1}$$

where u_1 and u_2 are the scalar valued control inputs, $V > 0$ and $\gamma_c \in (0, 0.79)$ are constants, $g > 0$ is a constant, and the state space is $\mathbb{R}^4 \times \left(-\frac{\pi}{2}, \frac{\pi}{2}\right)$. The available outputs are

$$\begin{cases} y_1(t) = \frac{\cos(\gamma_c)}{V}\eta(t)q_1(\mathcal{D}(t)), \quad y_2(t) = \frac{1}{V}\eta(t)q_2(\mathcal{D}(t)), \\ y_3(t) = \gamma(t), \quad y_4(t) = \psi(t), \quad y_5(t) = \phi(t) \end{cases} \tag{2}$$

where η is an unknown piecewise continuous function such that $\eta(t) \in [\underline{\eta}, \overline{\eta}]$ for all $t \geq 0$, with $\underline{\eta} > 0$ and $\overline{\eta} > \underline{\eta}$ being known constants, the unknown piecewise continuous nondecreasing right continuous $\mathcal{D} : \mathbb{R} \to \mathbb{R}$ admits a known constant $\overline{\mathcal{D}} \geq 0$ such that $t - \overline{\mathcal{D}} \leq \mathcal{D}(t) \leq t$ for all $t \geq 0$ and so can model measurement delays and sampling (e.g., by choosing $\mathcal{D}(t) = t - \overline{\mathcal{D}}$, or $\mathcal{D}(t) = t_i$ for all $\in [t_i, t_{i+1})$ for all $i \geq 0$, where $t_0 = 0$ and the sample times $t_i \geq 0$ admit a

constant $\epsilon_0 > 0$ such that $\overline{\mathcal{D}} \geq t_{i+1} - t_i \geq \epsilon_0$), and where $\cos(\gamma_c)$ was inserted in (2) to simplify a change of variables that we use below; see Remark 1 and Section II-B1 for a justification for the bound 0.79 on γ_c, and see Section III where (1)-(2) are shown to arise in the vision based landing of an airliner, where $\mathcal{D}$ incorporates the sampling and delay from image processing. We assume that the initial functions are constant at the initial time $t_0 = 0$, so $q_i(t) = q_i(0)$ for all $t \leq 0$ for $i = 1, 2$ and similarly for the other states.

The changes of coordinates

$$x_1 = \frac{\cos(\gamma_c) q_1}{V}, \quad x_2 = \frac{1}{V} q_2, \quad \text{and} \quad x_3 = \gamma - \gamma_c \tag{3}$$

and the fact that $\dot{x}_1 = \sin(\gamma - \gamma_c) + \cos(\gamma)\sin(\gamma_c)(1 - \cos(\psi))$ give the output component formulas $(y_1(t), y_2(t)) = \eta(t)(x_1(\mathcal{D}(t)), x_2(\mathcal{D}(t)))$ and

$$\begin{cases} \dot{x}_1 = \sin(x_3) + \cos(x_3 + \gamma_c)\sin(\gamma_c)[1 - \cos(\psi)], \quad \dot{x}_2 = \cos(x_3 + \gamma_c)\sin(\psi), \\ \dot{x}_3 = u_1, \quad \dot{\psi} = \frac{g}{V}\tan(\phi), \quad \dot{\phi} = u_2. \end{cases} \tag{4}$$

When $\eta(t)$ is known and differentiable, (4) can be globally asymptotically stabilized by a classical backstepping approach, whose first step requires the stabilization of $\dot{x}_1 = \sin(\nu_1) + \cos(\nu_1 + \gamma_c)\sin(\gamma_c)[1 - \cos(\nu_2)]$, $\dot{x}_2 = \cos(\nu_1 + \gamma_c)\sin(\nu_2)$ with ν_1 and ν_2 as the inputs followed by the addition of integrators [23]. However, neither classical backstepping nor other known results would apply to the stabilization problem we study here, where $\eta(t)$ is not known and possibly not differentiable. This motivates the new control design in the following theorem (where the consistency of our conditions on the constants and the justification for our choices of the constants are shown in Remark 1):

Theorem 1. Let $V > 0$, $g > 0$, $c_1 > 0$, and $c_2 > 0$ be constants, and η be a piecewise continuous function such that $\eta(t) \in [\underline{\eta}, \overline{\eta}]$ for all $t \geq 0$, with $\underline{\eta} > 0$ and $\overline{\eta} > \underline{\eta}$ being known constants. Let $\overline{\mathcal{D}}$, $\gamma_c \in (0, 0.79)$, τ, q_0, ς_i for $i = 1, 2, 3$, r_1, l_1, and l_2 be positive constants such that

$$l_1 l_2 < \tfrac{1}{8}, \tag{5}$$

$$2\overline{\eta} l_1 \leq r_1 \cos(\gamma_c), \tag{6}$$

$$\overline{\eta}\left(3 l_1 l_2 \left[\frac{2}{r_1} + \overline{\mathcal{D}}\right] + 2\overline{\mathcal{D}}\right) < l_2 \cos(\gamma_c), \tag{7}$$

$$4\left(\frac{\overline{\eta}\overline{\mathcal{D}}}{\cos(\gamma_c)}\right)^2 l_1\left(\frac{l_1}{\cos(\gamma_c)}+\frac{r_1}{\underline{\eta}}\right)<\cos(\gamma_c), \tag{8}$$

$$\varsigma_1\varsigma_2\leq\frac{\pi}{4}, \tag{9}$$

$$\varsigma_1\varsigma_3\overline{\eta}(2\tau+\overline{\mathcal{D}})<1, \text{ and} \tag{10}$$

$$2\pi(q_0\overline{\eta})^4\left(2\tau+\overline{\mathcal{D}}\right)^3\left(\tau+\overline{\mathcal{D}}\right)(c_\triangle\tau\varsigma_1\varsigma_3)^2<\sqrt{2}\underline{\eta}^2 \tag{11}$$

are all satisfied, where $c_\triangle=\frac{1}{(1-e^{-q_0\tau})^2}$. Let $\mathcal{D}$ be a piecewise continuous nondecreasing right continuous function such that $t-\overline{\mathcal{D}}\leq\mathcal{D}(t)\leq t$ for all $t\geq 0$. Choose the controls

$$u_1(t) = \frac{-r_1\left(\sin(\text{sat}_{\pi/3}(x_3(t)))+l_1\text{sat}_{l_2}(y_1(t)/\cos(\gamma_c))\right)}{\cos(\text{sat}_{\pi/3}(x_3(t)))} \text{ and} \tag{12}$$

$$\begin{aligned} u_2(t) = {} & \frac{\frac{V}{g}}{1+\tan^2(\phi(t))}\big[-(c_1+c_2)\tfrac{g}{V}\tan(\phi(t))-c_1c_2\psi(t)+c_2c_1\mathcal{F}(t) \\ & +(c_1+c_2)\mathcal{G}(t)+\mathcal{H}(t,z_{1,t},z_{2,t},x_{2,t})\big] \end{aligned} \tag{13}$$

in (4), where $(\mathcal{F},\mathcal{G},z_1,z_2)$ is the solution of

$$\begin{cases} \dot{\mathcal{F}}(t)=\mathcal{G}(t), \quad \dot{\mathcal{G}}(t)=\mathcal{H}(t,z_{1,t},z_{2,t},x_{2,t}), \\ \dot{z}_1(t)=q_0[-z_1(t)+z_2(t)], \quad \dot{z}_2(t)=q_0\left[-z_2(t)-\sigma_\dagger(y_2(t))\right] \end{cases} \tag{14}$$

that satisfies $(\mathcal{F},\mathcal{G},z_1,z_2)(0)=0$, and where

$$\begin{aligned} & \mathcal{H}(t,z_{1,t},z_{2,t},x_{2,t}) \\ & =c_\triangle q_0^2\big[z_1(t)-2z_2(t)-2e^{-q_0\tau}z_1(t-\tau)+e^{-2q_0\tau}z_1(t-2\tau)-\sigma_\dagger(y_2(t)) \\ & +2e^{-q_0\tau}\sigma_\dagger(y_2(t-\tau))-e^{-2q_0\tau}\sigma_\dagger(y_2(t-2\tau))+4e^{-q_0\tau}z_2(t-\tau)-2e^{-2q_0\tau}z_2(t-2\tau)\big] \end{aligned} \tag{15}$$

and $(y_1(t),y_2(t))=\eta(t)(x_1(\mathcal{D}(t)),x_2(\mathcal{D}(t)))$ and $\sigma_\dagger(p)=\varsigma_1\text{sat}_{\varsigma_2}(\varsigma_3 p)$ for all $p\in\mathbb{R}$. Then (4) in closed loop with (12)-(13) is globally asymptotically stable to 0 on its state space $\mathbb{R}^4\times\left(-\frac{\pi}{2},\frac{\pi}{2}\right)$. □

Remark 1. For any choices of $\gamma_c\in(0,0.79)$ and any positive constants q_0, τ, $\overline{\eta}$, r_1, $\overline{\mathcal{D}}$, and $\underline{\eta}\in(0,\overline{\eta})$, we can satisfy (5)-(11) by choosing the positive constants ς_i small enough, and choosing $l_1=l_0/n$ and $l_2=n$ for a large enough $n\in\mathbb{N}$ and a small enough constant $l_0>0$ (where the constant l_0 has been introduced to ensure that both l_1 and the product l_1l_2 are small enough and that l_2 is large enough to satisfy (5)-(8)). Therefore, (5)-(11) do not produce any

restrictions on the model parameters. See our appendix below for the derivation of the first two equalities in (14) from the formulas (27). Our choices of the constants $1/8$ and $\pi/4$ in (5) and (9) are justified in Section II-B1 as being called for to provide suitable asymptotic bounds on $\dot{x}_3$ and x_3, respectively; see the discussion of (19) below. Our upper bound 0.79 on γ_c is only used in Section II-B1 to ensure the lower bound $\cos\left(\arcsin(1/4)+\gamma_c\right) \geq \frac{1}{2}$ and so can be replaced by any bound $\bar{\gamma}_c \in (0, 0.79)$. The choices of the other constants in (5)-(11) are needed to apply our asymptotic convergence analysis under the preceding choices of the other constants. □

B. *Proof of Theorem 1*

1) Preliminary Step: Our strategy for proving Theorem 1 is to show how our control formulas (12)-(13) follow as solutions to two stabilization problems that correspond to suitable subsystems of (4). To this end, we use the changes of feedback

$$u_1 = \frac{-r_1 \sin(\sigma_1(x_3))+v_1}{\cos(\sigma_1(x_3))} \text{ and } u_2 = \frac{V}{g}\frac{u_3}{1+\frac{V^2}{g^2}x_4^2}, \tag{16}$$

where $x_4 = \frac{g}{V}\tan(\phi)$, $r_1 > 0$ is a constant that we further specify below,

$$\sigma_1 = \text{sat}_{\frac{\pi}{3}}, \text{ and } |v_1|_\infty < \frac{r_1}{8}. \tag{17}$$

The variable $x_4 = \frac{g}{V}\tan(\phi)$ on our state space where $\phi \in \left(-\frac{\pi}{2}, \frac{\pi}{2}\right)$ transforms (4) into

$$\begin{cases} \dot{x}_1 = \sin(x_3) + \cos(x_3+\gamma_c)\sin(\gamma_c)(1-\cos(\psi)), \quad \dot{x}_3 = \frac{-r_1\sin(\sigma_1(x_3))+v_1}{\cos(\sigma_1(x_3))}, \\ \dot{x}_2 = \cos(x_3+\gamma_c)\sin\psi, \quad \dot{\psi} = x_4, \quad \dot{x}_4 = \frac{g}{V}\left(1+\frac{V^2}{g^2}x_4^2\right)u_2 \ = \ u_3 \end{cases} \tag{18}$$

whose state space is $\mathbb{R}^5$. Hence, if we can find a globally asymptotically stabilizing feedback (v_1, u_3) for the origin of (18), then we will have obtained a feedback that ensures that $\mathbb{R}^4 \times \left(-\frac{\pi}{2}, \frac{\pi}{2}\right)$ is the basin of attraction for the origin of (4).

We will choose u_3 to be a linear function of the state of (18) plus a function of t and z_t where z is from our dynamical extension (14). Therefore, (18) will be forward complete because its nonlinear terms will be bounded. We next show how any solution of (18) on $[0, \infty)$ is such that $x_3(t)$ enters $\left[-\arcsin(\frac{1}{4}), \arcsin(\frac{1}{4})\right]$ in finite time. For each $t \geq 0$ such that $x_3(t) \geq \arcsin(\frac{1}{4})$, we can deduce from our bound on v_1 from (17) that

$$\dot{x}_3(t) \leq \frac{-r_1\sin(\sigma_1(\arcsin(\frac{1}{4})))+v_1}{\cos(\sigma_1(x_3(t)))} \leq -r_1\sin(\sigma_1(\arcsin(\tfrac{1}{4})))+\frac{|v_1|}{\cos(\sigma_1(x_3(t)))} \leq -\tfrac{r_1}{4}+2|v_1|_\infty < 0, \tag{19}$$

where the first inequality in (19) used the facts that $\pi/3 \geq \sigma_1(x_3(t)) \geq \sigma_1(\arcsin(1/4)) = \arcsin(1/4)$ (by (17)), that $\sin$ is nondecreasing on $[\arcsin(1/4), \pi/3]$, and that $\cos(s) \in (0,1]$ for all $s \in [\arcsin(1/4), \pi/3]$; the second inequality used the fact that $\cos$ is bounded above by 1; the third inequality used the facts that $\sigma_1(\arcsin(1/4)) = \arcsin(1/4)$ and $1 \geq \cos(\sigma_1(x_3(t))) \geq \cos(\pi/3) = 1/2$; and the last inequality used our bound on v_1 from (17). Similarly, if $x_3(t) \leq -\arcsin(\frac{1}{4})$, then $\dot{x}_3(t) \geq \frac{r_1}{4} - 2|v_1|_\infty > 0$. This provides a function $t_a \in \mathcal{K}_\infty$ such that for all $t \geq t_a(|x_3(0)|)$, we have $x_3(t) \in [-\arcsin(\frac{1}{4}), \arcsin(\frac{1}{4})]$. Therefore, $\cos(x_3(t) + \gamma_c) \geq \cos\left(\arcsin(1/4) + \gamma_c\right) \geq \frac{1}{2}$ for all $t \geq t_a(|x_3(0)|)$, because of our condition $\gamma_c \in (0, 0.79)$.

The preceding observations imply that if we can find controls u_3 and v_1 to uniformly globally exponentially stabilize the origin of

$$\dot{x}_2 = \varpi(t)\sin(\psi), \quad \dot{\psi} = x_4, \quad \dot{x}_4 = u_3 \tag{20}$$

for any continuous function $\varpi : [0,\infty) \to \left[\frac{1}{2}, 1\right]$ (with an exponential stability estimate that is independent of ϖ) and uniformly globally asymptotically stabilize the origin of

$$\dot{x}_1 = \sin(x_3) + d_1(t), \quad \dot{x}_3 = \frac{-r_1 \sin(\sigma_1(x_3)) + v_1}{\cos(\sigma_1(x_3))} \tag{21}$$

where d_1 is a state component of a uniformly globally exponentially stable system that satisfies $|d_1|_\infty \leq 2$, then we can globally asymptotically stabilize the origin of (1) with $\mathbb{R}^4 \times \left(-\frac{\pi}{2}, \frac{\pi}{2}\right)$ as its state space (by specializing our analysis of (21) to the function $d_1(t) = \cos(x_3(t) + \gamma_c)\sin(\gamma_c)(1 - \cos(\psi(t)))$). Hence, we devote the remainder of this section to the preceding asymptotic stabilization problems for (20) and (21) using our available output measurements (2), which will lead to our controls u_1 and u_2 from Theorem 1.

2) Stabilization of (21): By Section II-B1, we have (21) with $\sigma_1(x_3)$ replaced by x_3 for all times $t \geq t_a(|x_3(0)|)$. We next use $Z_1 = \sin(x_3)$ to obtain

$$\dot{x}_1 = Z_1 + d_1(t), \quad \dot{Z}_1 = -r_1 Z_1 + v_1 \tag{22}$$

where v_1 will be a function of $y_1(t) = \eta(t)x_1(\mathcal{D}(t))$. Then, v_1 is found in the following result which we prove in our appendix, which leads to $u_1(t)$ from (12) by substituting (23) into (16):

Theorem 2. Let r_1, l_1, and l_2 be positive constants such that (5)-(8) hold. Assume that d_1 in

(22) is a component of the state of a dynamics for a variable d that are uniformly globally exponentially stable to 0 and $|d_1|_\infty \leq 2$. Then the dynamics for (x_1, Z_1, d) in closed loop with

$$v_1 = -r_1 l_1 \mathrm{sat}_{l_2}(y_1/\cos(\gamma_c)) \tag{23}$$

are uniformly globally asymptotically stable to 0. □

3) Stabilization of (20): Using $\psi = \psi_1$, $\psi_2 = x_4 + c_1\psi$, and

$$u_3 = -(c_1 + c_2)x_4 - c_1c_2\psi_1 + v_3, \tag{24}$$

we obtain the dynamics

$$\dot{x}_2 = \varpi(t)\sin(\psi_1), \quad \dot{\psi}_1 = -c_1\psi_1 + \psi_2, \quad \dot{\psi}_2 = -c_2\psi_2 + v_3 \tag{25}$$

with the control v_3 being a function of the output $y_2(t) = \eta(t)x_2(\mathcal{D}(t))$. Then, v_3 is designed by the following result that we prove in our appendix below, which produces the desired uniformly globally exponentially stability result for (20) because of our choices of the change of variables and change of feedback, and which therefore leads to the control u_2 from (13) by substituting (26) in (24) and then substituting (24) into (16):

Theorem 3. Let $c_1 > 0$ and $c_2 > 0$ be constants. Let τ, q_0 and ς_i for $i = 1, 2, 3$ be positive constants such that (9)-(11) are satisfied, where $c_\triangle = \frac{1}{(1-e^{-q_0\tau})^2}$ and $\sigma_\dagger$ are as defined in the statement of Theorem 1. Choose the control

$$v_3(t) = c_2c_1\mathcal{F}(t) + (c_1 + c_2)\mathcal{G}(t) + \mathcal{H}(t, z_{1,t}, z_{2,t}, x_{2,t}) \text{ where} \tag{26}$$

$$\begin{aligned} \mathcal{F}(t) &= c_\triangle\left[z_1(t) - 2e^{-q_0\tau}z_1(t-\tau) + e^{-2q_0\tau}z_1(t-2\tau)\right] \text{ and} \\ \mathcal{G}(t) &= c_\triangle q_0\big[-z_1(t) + z_2(t) + 2e^{-q_0\tau}(z_1(t-\tau) - z_2(t-\tau)) \\ &\quad + e^{-2q_0\tau}(-z_1(t-2\tau) + z_2(t-2\tau))\big] \end{aligned} \tag{27}$$

and $\mathcal{H}$ is defined by (15) and where the z_i's are the states of the dynamic extension from (14) with the initial state $z(0) = 0$. Then $\dot{\mathcal{F}}(t) = \mathcal{G}(t)$ and $\dot{\mathcal{G}}(t) = \mathcal{H}(t, z_{1,t}, z_{2,t}, x_{2,t})$ hold for all $t \geq 0$, and we can construct constants $G_* > 0$ and $R_* > 0$ such that for all solutions (x_2, ψ_1, ψ_2) of (25) and all continuous functions $\varpi : [0, \infty) \to \left[\frac{1}{2}, 1\right]$, we have $|(x_2(t), \psi_1(t), \psi_2(t))| \leq$

$G_* e^{-R_* t} |(x_2(0), \psi_1(0), \psi_2(0))|$ for all $t \geq 0$. □

III. Illustration

We show how (1) from Section II arise when analyzing the align phase when an autopilot system must maintain a constant glide slope $\gamma_c = 3\text{deg}$ and align the aircraft with the runway axis at a constant airspeed $V = 70\text{ms}^{-1}$. Let Δ_X, Δ_Y, and Δ_Z denote the vector components between the aircraft center of gravity and the runway touchdown point; see Figure 1.

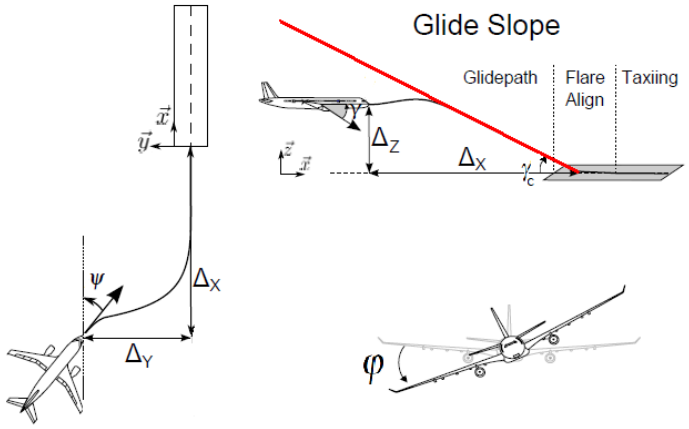


Fig. 1. Landing phases

The velocity vector is given by $\dot{\Delta}_X = V\cos(\gamma)\cos(\psi)$, $\dot{\Delta}_Y = V\cos(\gamma)\sin(\psi)$, and $\dot{\Delta}_Z = V\sin(\gamma)$, where γ (resp., ψ) is the aircraft vertical slope (resp., yaw difference between the aircraft speed and the runway axis). In addition, we have $\dot{\gamma} = u_1$, $\dot{\psi} = \frac{g}{V}\tan(\phi)$, and $\dot{\phi} = u_2$, in which ϕ is the aircraft roll angle, $g = 9.81\text{m.s}^{-2}$ is the local gravity, and $(u_1, u_2)^T$ is the guidance control input vector. The fastest loops are neglected in this study. The glide slope phase consists of tracking the line defined by $\Delta_Z^c = \tan(\gamma_c)\Delta_X$, and the deviations are computed as

$$q_1 = \Delta_Z - \Delta_Z^c \text{ and } q_2 = \Delta_Y. \tag{28}$$

Then $\dot{q}_1 = V\big(\sin(\gamma) - \cos(\gamma)\cos(\psi)\tan(\gamma_c)\big)$ holds. Combining the preceding equations shows that the deviation dynamics produce our system (1). We next show how our outputs (2) also arise from the preceding aircraft scenario.

To explain how we also obtain the outputs (2), consider the vision based control problem that was the focus of the ANR funded project VISIOLAND, in which the most stringent situation

(from the control viewpoint) was the vision based landing of an aircraft on an unequipped runway where the size of the runway is unknown.[1] More precisely, the runway is unequipped, so there are no landing ground facilities such as the Instrument Landing System (ILS) or the Global Positioning System (GPS). Hence, the automatic guidance loop must instead only rely on embedded sensors, which in this scenario were a monocular camera and an Inertial Measurement Unit (IMU). Assuming that the runway is not inclined, the relative attitude angles $y_3 = \gamma$ and $y_5 = \phi$ are the aircraft's slope and roll angles, which are given by the IMU. Let w denote the runway width, and assume that the runway is kept inside the camera field of view throughout the descent. In this case, it is shown in [24] that the relative yaw angle $y_4 = \psi$ and the outputs

$$y_{\text{image},1} = -\frac{\Delta_Z}{\Delta_X}, \quad y_{\text{image},2} = -\frac{w}{\Delta_X}, \quad y_{\text{image},3} = -\frac{\Delta_Y}{\Delta_X} \tag{29}$$

can be computed by applying image processing and a 'derotation' transformation to each image given by the body fixed camera, which produces delays and sampling. Let $\hat{w}$ denote a rough estimate of w, which can be either a saturated output of a width estimator [19] or a constant value that is chosen in the standard interval $[30\text{m}, 60\text{m}]$. Let $\eta = \frac{\hat{w}}{w}$. Then the required outputs y_1 and y_2 in (2) can be computed from the definitions (28)-(29) as follows:

$$y_1 = \frac{\cos(\gamma_c)\eta}{V} q_1 = \frac{\cos(\gamma_c)\hat{w}}{V y_{\text{image},2}} \big(y_{\text{image},1} + \tan(\gamma_c)\big) \text{ and } y_2 = \frac{\eta}{V} q_2 = \frac{\hat{w}}{V y_{\text{image},2}} y_{\text{image},3} \tag{30}$$

We next illustrate the use of our controls from Theorem 1 using $\overline{\eta} = \frac{4}{3}$ and $\underline{\eta} = \frac{2}{3}$.

To specify the longitudinal control law parameters, recall the control law (12), which was obtained from (16) and (23), with the constant $\overline{\mathcal{D}} \geq 0$ and the positive constants $\overline{\eta}$, $\underline{\eta}$, r_1, l_1, and l_2 satisfying (5)-(8). We thus propose to use the parameter values $r_1 = 3$, $l_1 = 0.15$, $l_2 = 0.8$, and $\overline{\mathcal{D}} = 150\text{ms}$, which satisfy (5)-(8) when $\overline{\eta} = \frac{4}{3}$ and $\underline{\eta} = \frac{2}{3}$. Recall that $\overline{\mathcal{D}} = 150\text{ms}$ represents the maximum amount of time to acquire and process an image; such a value seems reasonable since, once correctly initiated, the computer vision algorithm must simply track the runway (which is a trapezoid) in the image. To specify the lateral control law parameters, recall that the dynamical law is given by (13) from Theorem 1. Let us also recall that the constant $\overline{\mathcal{D}} \geq 0$ and

[1] See http://w3.onera.fr/visioland/node/92. Several cases can lead to this situation, such as an emergency landing on an unknown runway, a runway database failure or the difficulty of certifying such a database. The Visioland project aimed to be robust to commonly used databases and external positioning systems.

the positive constants τ, q_0, ς_1, ς_2, ς_3, $\overline{\eta}$, and $\underline{\eta}$ must satisfy (9)-(11). For our illustration, we chose the parameter values $c_1 = 0.6$, $c_2 = 0.6$, $\varsigma_1 = 0.003$, $\varsigma_2 = 78.5$, $\varsigma_3 = 11.5$, $q_0 = 0.5$, and $\tau = 1$. For this set of parameters, we now compute the maximum value of $\overline{\mathcal{D}}$ such that (9)-(11) are satisfied when $\overline{\eta} = \frac{4}{3}$ and $\underline{\eta} = \frac{2}{3}$, to obtain $\overline{\mathcal{D}} = 100$ms.

We performed a numerical simulation starting from the initial state $\psi(0) = 45$deg (which is sufficiently large so that the nonlinear coupling terms cannot be neglected). Choosing $\overline{\mathcal{D}} = 100$ms and the preceding values for the other constants, we assume that the outputs are sampled and delayed using $\mathcal{D}(t) = t_i$ for all $t \in [t_i, t_{i+1})$ and all integers $i \geq 0$, where $t_{i+1} - t_i = \overline{\mathcal{D}}$ for all $i \geq 0$ and $t_0 = 0$. We consider several constant values for η, and the time-varying case where $\eta(t) = 1 - 0.33e^{-0.1t}$. We present the results in Figures 2 and 3, which show that the proposed control laws are able to stabilize the aircraft on its glide slope for all of the studied η values. We plotted an approximation of the load factor $N_z \cong \frac{V}{g}u_1 + \frac{\cos(\gamma)}{\cos(\phi)}$ in place of u_1 in the longitudinal frame. Since our simulations exhibit good performance, they help to validate our theory for the preceding dynamics.

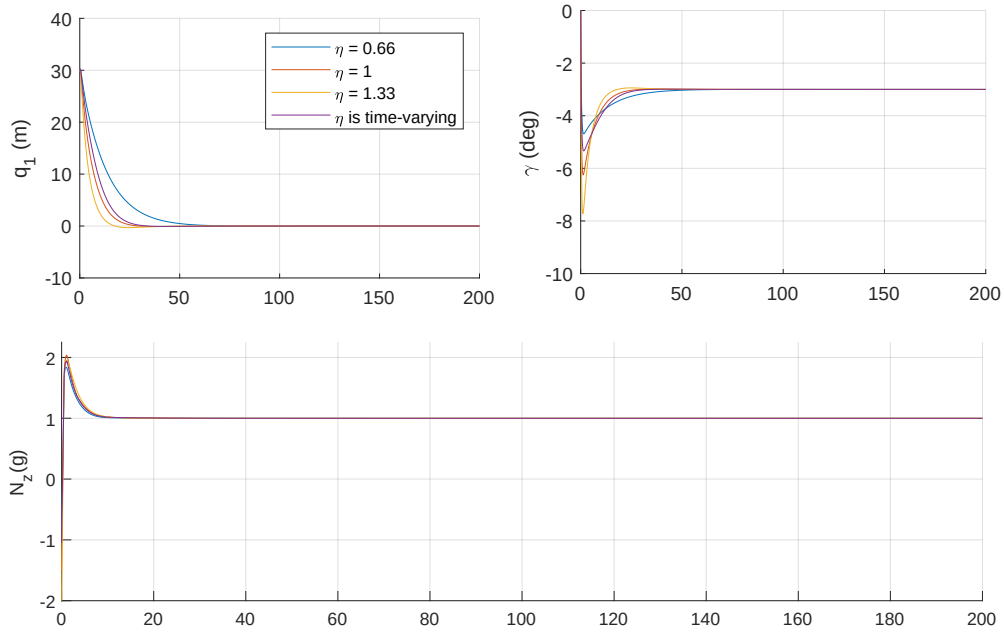


Fig. 2. Longitudinal states evolution

IV. Conclusion

We applied a new backstepping approach to solve a nontrivial visual servoing control design problem. Our finite dimensional dynamic extension circumvents the problem posed by the use of

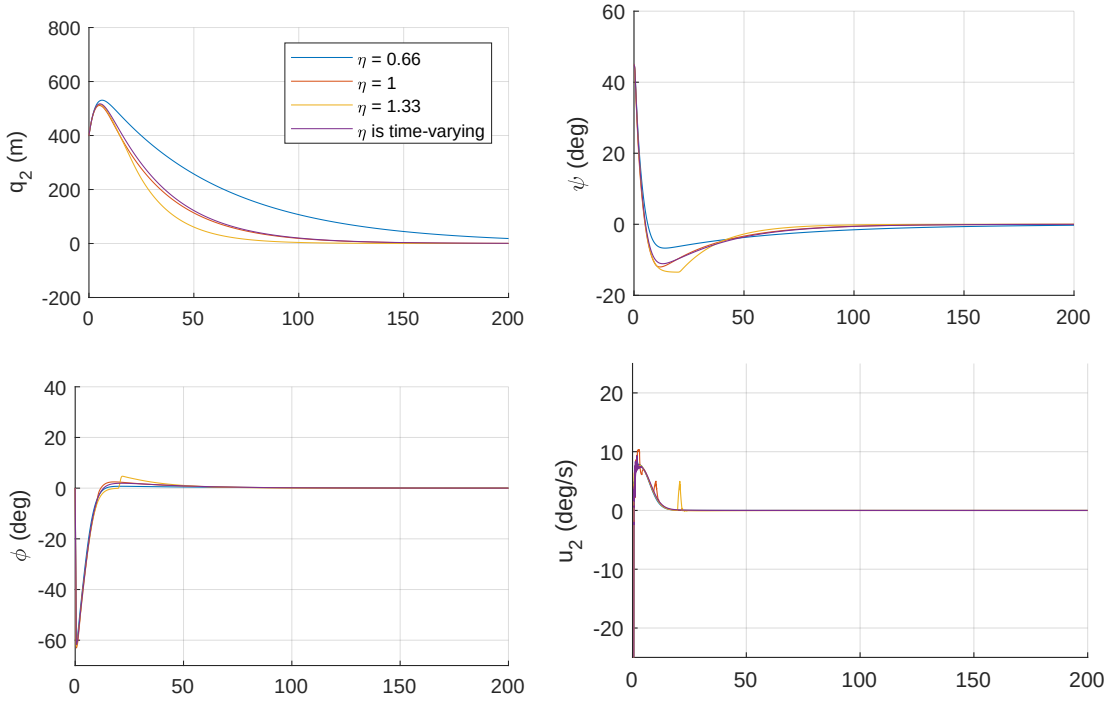


Fig. 3. Lateral states and lateral control evolution

visual measurements. Indeed, classical backstepping requires the successive pseudo-controllers to be sufficiently smooth which was not the case in our application. We allow the use of sampled and delayed visual information, to take the image processing into account in our design.

APPENDIX: PROOFS OF THEOREMS 2-3

We prove Theorems 2-3 from Section II-B. In what follows, we use the fact that for all continuous functions $\phi : \mathbb{R} \to [0, \infty)$ and constants $\bar{\tau} > 0$, the following hold for all $t \in \mathbb{R}$:

$$\tfrac{d}{dt} \int_{t-\overline{\tau}}^{t} \int_{s}^{t} \phi(\ell) \mathrm{d}\ell \mathrm{d}s = \overline{\tau}\phi(t) - \int_{t-\overline{\tau}}^{t} \phi(\ell)\mathrm{d}\ell \quad \text{and} \quad \int_{t-\overline{\tau}}^{t} \int_{s}^{t} \phi(\ell)\mathrm{d}\ell\mathrm{d}s \leq \overline{\tau} \int_{t-\overline{\tau}}^{t} \phi(\ell)\mathrm{d}\ell, \tag{31}$$

where the equality followed from Fubini's theorem. We also set $c_{**} = c_{\triangle}^2 q_0^4 c_* \tau^2 (1+\epsilon)^2 (2\tau + \bar{\mathcal{D}})^2$, where $c_* = \varsigma_1 \varsigma_3 \overline{\eta}^2 (2\tau + \bar{\mathcal{D}})/(2\underline{\eta})$ and fix a constant $\epsilon \in (0, 1)$ that is small enough such that

$$\overline{\eta} \left(\tfrac{6 l_1 l_2}{r_1} (1+\epsilon)^2 + 3\overline{\mathcal{D}} l_1 l_2 (1+\epsilon)^2 + 2\overline{\mathcal{D}} \right) < l_2 \cos(\gamma_c), \tag{32a}$$

$$\left(\tfrac{(1+\epsilon)\overline{\eta}\overline{\mathcal{D}}}{\cos(\gamma_c)} \right)^2 l_1 \left(\tfrac{l_1}{\cos(\gamma_c)} + (r_1/\underline{\eta}) \right) < \tfrac{\cos(\gamma_c)}{4}, \tag{32b}$$

$$(1+\epsilon)\varsigma_1 \varsigma_3 \overline{\eta} \big(2\tau + \overline{\mathcal{D}} \big) < 1, \quad \text{and} \tag{32c}$$

$$2\pi(\tau + \overline{\mathcal{D}})(1+\epsilon) c_{**} \overline{\eta}^2 \varsigma_1 \varsigma_3 < \sqrt{2}(1-\epsilon)\underline{\eta} \tag{32d}$$

and where we can satisfy (32a)-(32d) for some $\epsilon \in (0,1)$ by (7), (8), (10), and (11), respectively.

Proof of Theorem 2. The system (22) in closed loop with the control from Theorem 2 is

$$\dot{x}_1(t) = Z_1(t) + d_1(t), \quad \dot{Z}_1(t) = -r_1 \left[Z_1(t) + \sigma_3(\eta(t) x_1(\mathcal{D}(t))) \right], \tag{33}$$

where $\sigma_3(\ell) = l_1 \mathrm{sat}_{l_2}(\ell / \cos(\gamma_c))$. The new variable $m(t) = x_1(t) + \frac{1}{r_1} Z_1(t)$ produces

$$\begin{cases} \dot{m}(t) = -\sigma_3 \left(\eta(t) \left(m(t) - \frac{1}{r_1} Z_1(t) + \Delta x_1(t) \right) \right) + d_1(t) \\ \dot{Z}_1(t) = r_1 \left[-Z_1(t) - \sigma_3 \left(\eta(t) \left(m(t) - \frac{1}{r_1} Z_1(t) \right) \right) \right] + \Delta_\sigma(t), \end{cases} \tag{34}$$

where $\Delta_\sigma(t) = -r_1 [\sigma_3(\eta(t) x_1(\mathcal{D}(t))) - \sigma_3(\eta(t) x_1(t))]$ and $\Delta x_1(t) = x_1(\mathcal{D}(t)) - x_1(t)$.

Since $|\Delta_\sigma|_\infty \leq 2 r_1 l_1 l_2$, it is easy to see that there exists a function $t_b \in \mathcal{K}_\infty$ such that

$$|Z_1(t)| \leq 3 l_1 l_2 (1 + \epsilon) \tag{35}$$

for all $t \geq t_b(|(x_1(0), Z_1(0))|)$, because $\dot{Z}_1(t) > 0$ (resp., < 0) when $Z_1(t) < -3 l_1 l_2 (1+\epsilon)$ (resp., $> 3 l_1 l_2 (1+\epsilon)$) and σ_3 is bounded by $l_1 l_2$. This and (33) give $|\Delta x_1(t)| \leq \overline{\mathcal{D}} |\dot{x}_1|_{[t-\overline{\mathcal{D}}, t]} \leq \overline{\mathcal{D}}(3 l_1 l_2 (1+\epsilon) + 2)$ for all $t \geq t_b(|(x_1(0), Z_1(0))|) + \overline{\mathcal{D}}$ (since d_1 is bounded by 2), so since the d dynamics are uniformly globally exponentially stable to 0, we can use (34) to find a $t_c \in \mathcal{K}_\infty$ such that $t_c(p) \geq t_b(p)$ for all $p \geq 0$ and such that

$$|m(t)| \leq 3 l_1 l_2 (1+\epsilon)^2 \left[(1/r_1) + \overline{\mathcal{D}} \right] + 2\overline{\mathcal{D}} \tag{36}$$

for all $t \geq t_c(|(x_1(0), Z_1(0), d(0))|) + \overline{\mathcal{D}}$, by showing that $\dot{m}(t) < 0$ (resp., > 0) if $m(t) > \overline{m}$ (resp., $< -\overline{m}$) where $\overline{m}$ is the right side of (36), and recalling that η is bounded below by $\underline{\eta}$. This and (35) imply that for all $t \geq t_c(|(x_1(0), Z_1(0), d(0))|) + \overline{\mathcal{D}}$, we have

$$\eta(t) \left| m(t) - \tfrac{1}{r_1} Z_1(t) \right| \leq \overline{\eta} \left(\tfrac{6 l_1 l_2 (1+\epsilon)^2}{r_1} + 3\overline{\mathcal{D}} l_1 l_2 (1+\epsilon)^2 + 2\overline{\mathcal{D}} \right).$$

Therefore, (32a) gives $|\eta(t) (m(t) - Z_1(t)/r_1)| \leq l_2 \cos(\gamma_c)$ and so also

$$\sigma_3 \left(\eta(t) \left(m(t) - \tfrac{1}{r_1} Z_1(t) \right) \right) = \tfrac{l_1 \eta(t)}{\cos(\gamma_c)} \left(m(t) - \tfrac{1}{r_1} Z_1(t) \right) \tag{37}$$

for all $t \geq t_c(|(x_1(0), Z_1(0), d(0))|) + \overline{\mathcal{D}}$. This produces the system

$$\begin{cases} \dot{m}(t) = -\frac{l_1 \eta(t)}{\cos(\gamma_c)} \left(m(t) - \frac{1}{r_1} Z_1(t) \right) + d_1(t) + \Delta_\sigma^\sharp(t) \\ \dot{Z}_1(t) = r_1 \left[-Z_1(t) - \frac{l_1 \eta(t)}{\cos(\gamma_c)} \left(m(t) - \frac{Z_1(t)}{r_1} \right) \right] + \Delta_\sigma(t) \end{cases} \tag{38}$$

which we rewrite as

$$\left\{\begin{array}{l} \dot{m}(t) = -\frac{l_1\eta(t)m(t)}{\cos(\gamma_c)} + \frac{\eta(t)l_1}{r_1\cos(\gamma_c)}Z_1(t) + d_1(t) + \Delta_\sigma^\sharp(t) \\ \dot{Z}_1(t) = \left(\frac{l_1\eta(t)}{\cos(\gamma_c)} - r_1\right)Z_1(t) - \frac{r_1 l_1\eta(t)}{\cos(\gamma_c)}m(t) + \Delta_\sigma(t) \end{array}\right. \tag{39}$$

for all $t \geq t_c(|(x_1(0), Z_1(0), d(0))|) + \overline{\mathcal{D}}$, where

$$\Delta_\sigma^\sharp(t) \;=\; \sigma_3\left(\eta(t)\left(m(t) - \tfrac{1}{r_1}Z_1(t)\right)\right) - \sigma_3\left(\eta(t)\left(m(t) - \tfrac{1}{r_1}Z_1(t) + \Delta x_1(t)\right)\right). \tag{40}$$

We next analyze the stability of (39) using the candidate Lyapunov function $\nu(m, Z_1) = \frac{1}{2}\cos(\gamma_c)(r_1^2m^2 + Z_1^2)$. In the Lyapunov function analysis in the rest of this proof, we only consider values $t \geq t_c(|(x_1(0), Z_1(0), d(0))|)+\overline{\mathcal{D}}$. Then at the end of the proof, we also consider values $t \in [0, t_c(|(x_1(0), Z_1(0), d(0))|) + \overline{\mathcal{D}}]$. Elementary calculations give

$$\begin{aligned} \dot{\nu}(t) =& l_1 r_1^2 m(t)\left[-\eta(t)m(t) + \tfrac{\eta(t)}{r_1}Z_1(t) + \tfrac{\cos(\gamma_c)d_1(t)}{l_1}\right] + Z_1(t)\cos(\gamma_c)\Delta_\sigma(t) \\ &+ Z_1(t)[(l_1\eta(t) - \cos(\gamma_c)r_1)Z_1(t) - r_1 l_1\eta(t)m(t)] + r_1^2 m(t)\cos(\gamma_c)\Delta_\sigma^\sharp(t) \\ =& -l_1\eta(t)r_1^2m^2(t) + (\eta(t)l_1 - \cos(\gamma_c)r_1)Z_1^2(t) + \cos(\gamma_c)r_1^2m(t)d_1(t) \\ &+ r_1^2 m(t)\cos(\gamma_c)\Delta_\sigma^\sharp(t) + Z_1(t)\cos(\gamma_c)\Delta_\sigma(t). \end{aligned} \tag{41}$$

along all solutions of (39). By applying Young's inequality to obtain $\cos(\gamma_c)r_1^2m(t)d_1(t) \leq (\underline{\eta}l_1/2)r_1^2m^2(t) + (1/(2\underline{\eta}l_1))r_1^2d_1^2(t)$, we conclude from (6) and (41) that

$$\begin{aligned} \dot{\nu}(t) \;\leq\; & -\tfrac{\underline{\eta}l_1}{2}r_1^2m^2(t) - \tfrac{\cos(\gamma_c)r_1}{2}Z_1^2(t) + \tfrac{1}{2\underline{\eta}l_1}r_1^2d_1^2(t) + r_1^2m(t)\cos(\gamma_c)\Delta_\sigma^\sharp(t) \\ & + \cos(\gamma_c)Z_1(t)\Delta_\sigma(t). \end{aligned} \tag{42}$$

We next use Young's and Jensen's inequality to find upper bounds for $\cos(\gamma_c)r_1^2m(t)\Delta_\sigma^\sharp(t) + \cos(\gamma_c)Z_1(t)\Delta_\sigma(t)$ in (42). To this end, notice that we have

$$\begin{aligned} |Z_1(t)\Delta_\sigma(t)| \;\leq\; & \tfrac{r_1\cos(\gamma_c)}{4}Z_1^2(t) + \tfrac{1}{r_1\cos(\gamma_c)}\Delta_\sigma^2(t) \\ \leq\; & \tfrac{r_1\cos(\gamma_c)}{4}Z_1^2(t) + \tfrac{r_1}{\cos(\gamma_c)}\left(\tfrac{l_1\overline{\eta}}{\cos(\gamma_c)}\right)^2\left(\textstyle\int_{t-\overline{\mathcal{D}}}^t|\dot{x}_1(\ell)|\mathrm{d}\ell\right)^2 \\ \leq\; & \tfrac{r_1\cos(\gamma_c)}{4}Z_1^2(t) + \tfrac{r_1}{\cos(\gamma_c)}\left(\tfrac{l_1\overline{\eta}}{\cos(\gamma_c)}\right)^2\overline{\mathcal{D}}\textstyle\int_{t-\overline{\mathcal{D}}}^t|\dot{x}_1(\ell)|^2\mathrm{d}\ell \end{aligned}$$

and

$$\begin{aligned} |r_1^2m(t)\Delta_\sigma^\sharp(t)| \;\leq\; & \tfrac{\underline{\eta}l_1}{4}r_1^2m^2(t) + \tfrac{r_1^2}{\underline{\eta}l_1}\left(\Delta_\sigma^\sharp(t)\right)^2 \\ \leq\; & \tfrac{\underline{\eta}l_1}{4}r_1^2m^2(t) + \tfrac{r_1^2l_1^2\overline{\eta}^2}{\cos^2(\gamma_c)\underline{\eta}l_1}\left(\textstyle\int_{t-\overline{\mathcal{D}}}^t|\dot{x}_1(\ell)|\mathrm{d}\ell\right)^2 \\ \leq\; & \tfrac{\underline{\eta}l_1}{4}r_1^2m^2(t) + \tfrac{r_1^2l_1\overline{\eta}^2\overline{\mathcal{D}}}{\cos^2(\gamma_c)\underline{\eta}}\textstyle\int_{t-\overline{\mathcal{D}}}^t\dot{x}_1^2(\ell)\mathrm{d}\ell \end{aligned}$$

for all $t \geq 0$. Hence, the time derivative of

$$\nu^\sharp(m_t, Z_{1t}) = \nu\big(m(t), Z_1(t)\big) + r_1(1+\epsilon)\left(\tfrac{\overline{\eta}}{\cos(\gamma_c)}\right)^2 \overline{\mathcal{D}} l_1 \left(\tfrac{l_1}{\cos(\gamma_c)} + \tfrac{r_1}{\underline{\eta}}\right) \int_{t-\overline{\mathcal{D}}}^t \int_s^t \dot{x}_1^2(p)\mathrm{d}p\mathrm{d}s \tag{43}$$

along all solutions of (39) satisfies

$$\begin{aligned} \dot{\nu}^\sharp \;\leq\; & -\tfrac{\underline{\eta} l_1}{4} r_1^2 m^2(t) - \tfrac{r_1 \cos(\gamma_c)}{4} Z_1^2(t) + \tfrac{1}{2\underline{\eta} l_1} r_1^2 d_1^2(t) \\ & + r_1(1+\epsilon)\left(\tfrac{\overline{\eta}\overline{\mathcal{D}}}{\cos(\gamma_c)}\right)^2 l_1 \left(\tfrac{l_1}{\cos(\gamma_c)} + \tfrac{r_1}{\underline{\eta}}\right) \dot{x}_1^2(t) \\ & - r_1 \epsilon \left(\tfrac{\overline{\eta}}{\cos(\gamma_c)}\right)^2 \overline{\mathcal{D}} l_1 \left(\tfrac{l_1}{\cos(\gamma_c)} + \tfrac{r_1}{\underline{\eta}}\right) \int_{t-\overline{\mathcal{D}}}^t \dot{x}_1^2(\ell)\mathrm{d}\ell, \end{aligned} \tag{44}$$

where we used (31) with $\overline{\tau} = \overline{\mathcal{D}}$ and $\phi(s) = \dot{x}_1^2(s)$.

Since Young's inequality and our formula for $\dot{x}_1$ from (33) yield $(\dot{x}_1(t))^2 \leq (1+\epsilon) Z_1^2(t) + (1 + (1/\epsilon)) d_1^2(t)$ for all $t \geq 0$, we can then use (44) to find a constant $\bar{d} > 0$ such that

$$\begin{aligned} \dot{\nu}^\sharp \;\leq\; & -\tfrac{\underline{\eta} l_1}{4} r_1^2 m^2(t) + \bar{d} d_1^2 + \left[r_1 \left(\tfrac{(1+\epsilon)\overline{\eta}\overline{\mathcal{D}}}{\cos(\gamma_c)}\right)^2 l_1 \left(\tfrac{l_1}{\cos(\gamma_c)} + \tfrac{r_1}{\underline{\eta}}\right) - \tfrac{\cos(\gamma_c) r_1}{4} \right] Z_1^2(t) \\ & - r_1 \epsilon \left(\tfrac{\overline{\eta}}{\cos(\gamma_c)}\right)^2 l_1 \left(\tfrac{l_1}{\cos(\gamma_c)} + \tfrac{r_1}{\underline{\eta}}\right) \int_{t-\overline{\mathcal{D}}}^t \int_s^t \dot{x}_1^2(p)\mathrm{d}p\mathrm{d}s \end{aligned} \tag{45}$$

along all solutions of (39), by (31). By (32b), the quantity in square brackets in (45) is negative. Therefore, we can find positive constants $\bar{c}_0$ and $\bar{c}_1$ such that $\dot{\nu}^\sharp \leq -\bar{c}_0 \nu^\sharp(m_t, Z_{1t}) + \bar{c}_1 d_1^2(t)$ holds along all solutions of (39) for all times $t \geq t_c(|(x_1(0), Z_1(0), d(0))|) + \overline{\mathcal{D}}$. This and the quadratic upper and lower bounds of $\nu^\sharp$ and the fact that the nonlinear terms in the dynamics (39) grow linearly in the state provides an exponential input-to-state stability estimate for the (m, Z_1) dynamics with an overshoot of the form $\gamma(|d|_{[0,t]})$ for some $\gamma \in \mathcal{K}_\infty$ that is valid for all $t \geq 0$. The result now follows because the d dynamics are uniformly globally exponentially stable to 0, by standard small gain arguments [22].

Proof of Theorem 3. First notice that our definitions from Theorem 3 give $\dot{\mathcal{F}}(t) = \mathcal{G}(t)$,

$$c_\triangle = \frac{1}{(1-e^{-q_0\tau})^2} = \frac{1}{q_0^2 \int_{t-\tau}^t e^{q_0(m-t)} \int_{m-\tau}^m e^{q_0(\ell-m)} \mathrm{d}\ell \mathrm{d}m}, \text{ and} \tag{46}$$

$$\begin{aligned} \tfrac{\ddot{\mathcal{F}}(t)}{c_\triangle q_0} \;=\; & -\dot{z}_1(t) + \dot{z}_2(t) + 2e^{-q_0\tau}\dot{z}_1(t-\tau) - e^{-2q_0\tau}\dot{z}_1(t-2\tau) - 2e^{-q_0\tau}\dot{z}_2(t-\tau) + e^{-2q_0\tau}\dot{z}_2(t-2\tau) \\ =\; & q_0[z_1(t) - z_2(t)] + q_0[-z_2(t) - \sigma_\dagger(y_2(t))] \\ & - 2e^{-q_0\tau} q_0[z_1(t-\tau) - z_2(t-\tau)] + e^{-2q_0\tau} q_0[z_1(t-2\tau) - z_2(t-2\tau)] \\ & + 2e^{-q_0\tau} q_0[z_2(t-\tau) + \sigma_\dagger(y_2(t-\tau))] + e^{-2q_0\tau} q_0[-z_2(t-2\tau) - \sigma_\dagger(y_2(t-2\tau))] \end{aligned}$$

so $\ddot{\mathcal{F}}(t) = \mathcal{H}(t, z_{1,t}, z_{2,t}, x_{2,t})$ for all $t \in \mathbb{R}$. Set $\omega_1(t) = \psi_1(t) - \mathcal{F}(t)$ and $\omega_2(t) = \psi_2(t) -$

$(c_1\mathcal{F}(t)+\mathcal{G}(t))$. By our formulas (25)-(26) for the (x_2,ψ_1,ψ_2) dynamics and v_3, we obtain

$$\dot{x}_2(t)=\varpi(t)\sin\left(\mathcal{F}(t)+\omega_1(t)\right),\quad \dot{\omega}_1(t)=-c_1\omega_1(t)+\omega_2(t),\quad \dot{\omega}_2(t)=-c_2\omega_2(t). \tag{47}$$

Since the (ω_1,ω_2)-subsystem of (47) is exponentially stable, we now study

$$\begin{aligned}&\dot{x}_2(t)=\varpi(t)\sin\left(\mathcal{F}(t)\right)+\delta_1(t),\quad \dot{z}_1(t)=q_0[-z_1(t)+z_2(t)],\\&\dot{z}_2(t)=q_0\left[-z_2(t)-\sigma_\dagger(y_2(t))\right]\end{aligned} \tag{48}$$

with $\delta_1(t)=\varpi(t)\left(\sin\left(\mathcal{F}(t)+\omega_1(t)\right)-\sin\left(\mathcal{F}(t)\right)\right)$ satisfying $|\delta_1(t)|\leq|\omega_1(t)|$ for all $t\geq 0$ (by our bound 1 on ϖ) and with $z(0)=0$. By integrating the z-subsystem of (48), we obtain $z_2(t)=-q_0\int_0^t e^{q_0(\ell-t)}\sigma_\dagger(y_2(\ell))\mathrm{d}\ell$ and therefore also

$$\begin{aligned}z_1(t)-e^{-\tau q_0}z_1(t-\tau)&=q_0\int_{t-\tau}^t e^{q_0(m-t)}z_2(m)\mathrm{d}m\\&=-q_0^2\int_{t-\tau}^t e^{q_0(m-t)}\int_0^m e^{q_0(\ell-m)}\sigma_\dagger(y_2(\ell))\mathrm{d}\ell\mathrm{d}m\end{aligned} \tag{49}$$

when $t\geq\tau$. It follows from a simple change of variables that

$$\begin{aligned}z_1(t)-e^{-\tau q_0}z_1(t-\tau)&=-q_0^2\int_{t-\tau}^t e^{q_0(m-t)}\int_{m-\tau}^m e^{q_0(\ell-m)}\sigma_\dagger(y_2(\ell))\mathrm{d}\ell\mathrm{d}m\\&\quad -q_0^2\int_{t-2\tau}^{t-\tau} e^{q_0(s-t)}\int_0^s e^{q_0(\ell-s)}\sigma_\dagger(y_2(\ell))\mathrm{d}\ell\mathrm{d}s\\&=-q_0^2\int_{t-\tau}^t e^{q_0(m-t)}\int_{m-\tau}^m e^{q_0(\ell-m)}\sigma_\dagger(y_2(\ell))\mathrm{d}\ell\mathrm{d}m\\&\quad +e^{-q_0\tau}\left[-q_0^2\int_{t-2\tau}^{t-\tau} e^{q_0(s-t+\tau)}\int_0^s e^{q_0(\ell-s)}\sigma_\dagger(y_2(\ell))\mathrm{d}\ell\mathrm{d}s\right].\end{aligned} \tag{50}$$

Replacing t by $t-\tau$ in (49), and then using the result to replace the term in squared brackets in (50), and then collecting terms, we obtain

$$z_1(t)-2e^{-\tau q_0}z_1(t-\tau)+e^{-2q_0\tau}z_1(t-2\tau)=-q_0^2\int_{t-\tau}^t e^{q_0(m-t)}\int_{m-\tau}^m e^{q_0(\ell-m)}\sigma_\dagger(y_2(\ell))\mathrm{d}\ell\mathrm{d}m$$

for all $t\geq 2\tau$. From our formula (27) for $\mathcal{F}$, it follows that

$$\tfrac{\mathcal{F}(t)}{c_\triangle}=-q_0^2\int_{t-\tau}^t e^{q_0(m-t)}\int_{m-\tau}^m e^{q_0(\ell-m)}\sigma_\dagger(y_2(\ell))\mathrm{d}\ell\mathrm{d}m. \tag{51}$$

Therefore, (48) gives $\dot{x}_2(t)=\varpi(t)\sin(\xi(y_{2,t}))+\delta_1(t)$, where

$$\xi(y_{2,t})=c_\triangle\Big[-q_0^2\int_{t-\tau}^t\int_{m-\tau}^m e^{q_0(\ell-t)}\sigma_\dagger(y_2(\ell))\mathrm{d}\ell\mathrm{d}m\Big]. \tag{52}$$

From (9) and (46), we get $|\xi(y_{2,t})|\leq\varsigma_1\varsigma_2\leq\frac{\pi}{4}$ for all $t\geq 0$. We rewrite the x_2 dynamics as

$$\dot{x}_2(t)=\delta_1(t)-\theta(t)c_\triangle q_0^2\int_{t-\tau}^t\int_{m-\tau}^m e^{q_0(\ell-t)}\sigma_\dagger(\eta(\ell)x_2(\mathcal{D}(\ell)))\mathrm{d}\ell\mathrm{d}m \tag{53}$$

where $\theta(t) = \varpi(t)\sin(\xi(y_{2,t}))/\xi(y_{2,t})$ when $\xi(y_{2,t}) \neq 0$ and $\theta(t) = 1$ when $\xi(y_{2,t}) = 0$. Then, recalling that $\varpi(t) \in [1/2, 1]$ for all $t \geq 0$ and that $\sin(m)/m \in [2\sqrt{2}/\pi, 1]$ for all $m \in (0, \pi/4]$ (which follows because $\sin(m)/m$ is nonincreasing on $(0, \pi/4)$), we have $\theta(t) \in [\underline{\theta}, 1]$ for all $t \geq 0$, where $\underline{\theta} = \sqrt{2}/\pi$. From (53), we deduce that

$$\dot{x}_2(t) \;=\; -\theta(t)c_{\triangle}q_0^2 \int_{t-\tau}^{t}\int_{m-\tau}^{m} e^{q_0(\ell-t)}\sigma_{\dagger}\Big(\eta(\ell)x_2(t) + \eta(\ell)\int_{t}^{\mathcal{D}(\ell)} \dot{x}_2(s)\mathrm{d}s\Big)\mathrm{d}\ell\mathrm{d}m + \delta_1(t) \tag{54}$$

for all $t \geq 4\tau + \overline{\mathcal{D}}$. From the formula $c_{\triangle} = \frac{1}{(1-e^{-q_0\tau})^2}$ from (46), and also using our formula $\sigma_{\dagger}(p) = \varsigma_1 \mathrm{sat}_{\varsigma_2}(\varsigma_3 p)$ and (53), it follows that for all $\ell \in [t-2\tau, t]$, we have

$$\left|\int_{t}^{\mathcal{D}(\ell)} \dot{x}_2(s)\mathrm{d}s\right| \leq \left(2\tau + \overline{\mathcal{D}}\right)\left(\varsigma_1\varsigma_2 + |\omega_1|_{[t-2\tau-\overline{\mathcal{D}},t]}\right). \tag{55}$$

Then, since the ω dynamics are uniformly globally exponentially stable to 0, we deduce from (54)-(55) and (32c) that we can construct a $t_d \in \mathcal{K}_{\infty}$ such that $|x_2(t)| \leq (1+\epsilon)(2\tau + \overline{\mathcal{D}})\varsigma_1\varsigma_2$ for all $t \geq t_d(|(x_2(0), \omega(0))|) + 4\tau + 2\overline{\mathcal{D}}$, and so also $\sigma_{\dagger}(\eta(\ell)x_2(\mathcal{D}(\ell))) = \varsigma_1\varsigma_3\eta(\ell)x_2(\mathcal{D}(\ell))$ for all $\ell \geq t_d(|(x_2(0), \omega(0))|) + 4\tau + 2\overline{\mathcal{D}}$ because $(1+\epsilon)\varsigma_1\varsigma_2\varsigma_3\overline{\eta}(2\tau + \overline{\mathcal{D}}) < \varsigma_2$ and also using the fact that $\dot{x}_2(t) > 0$ (resp., < 0) if $x_2(t) < -(1+\epsilon)(2\tau + \overline{\mathcal{D}})\varsigma_1\varsigma_2$ (resp., $x_2(t) > (1+\epsilon)(2\tau + \overline{\mathcal{D}})\varsigma_1\varsigma_2$. Set $\varsigma_4 = \varsigma_1\varsigma_3$. Then, for all $t \geq t_d(|(x_2(0), \omega(0))|) + 6\tau + 2\overline{\mathcal{D}}$, we can use (53) to obtain

$$\begin{aligned}\dot{x}_2(t) \;&=\; \delta_1(t) - \theta(t)c_{\triangle}\varsigma_4 q_0^2 \int_{t-\tau}^{t}\int_{m-\tau}^{m} e^{q_0(\ell-t)}\eta(\ell)x_2(\mathcal{D}(\ell))\mathrm{d}\ell\mathrm{d}m \\ &=\; -\theta(t)c_{\triangle}\varsigma_4 q_0^2 \int_{t-\tau}^{t}\int_{m-\tau}^{m} e^{q_0(\ell-t)}\Big(\eta(\ell)x_2(t) + \eta(\ell)\int_{t}^{\mathcal{D}(\ell)} \dot{x}_2(s)\mathrm{d}s\Big)\mathrm{d}\ell\mathrm{d}m + \delta_1(t),\end{aligned} \tag{56}$$

by applying the Fundamental Theorem of Calculus to x_2.

Next note that the time derivative of $V_0(x_2) = \frac{1}{2}x_2^2$ along all trajectories of (56) satisfies

$$\begin{aligned}&\dot{V}_0(t) = -\theta(t)c_{\triangle}q_0^2\varsigma_4 \int_{t-\tau}^{t}\int_{m-\tau}^{m} e^{q_0(\ell-t)}\eta(\ell)\mathrm{d}\ell\mathrm{d}m x_2^2(t) \\ &-x_2(t)\theta(t)c_{\triangle}q_0^2\varsigma_4 \int_{t-\tau}^{t}\int_{m-\tau}^{m} e^{q_0(\ell-t)}\eta(\ell)\int_{t}^{\mathcal{D}(\ell)} \dot{x}_2(s)\mathrm{d}s\mathrm{d}\ell\mathrm{d}m + x_2(t)\delta_1(t).\end{aligned} \tag{57}$$

Here and in the rest of our Lyapunov functional analysis, we only consider those time values that satisfy $t \geq t_d(|(x_2(0), \omega(0))|) + 6\tau + 2\overline{\mathcal{D}}$, and then we consider smaller values $t \geq 0$ at the end to complete the proof. Using the definition of $\underline{\eta}$ and (46), we obtain

$$\begin{aligned}\dot{V}_0(t) \;\leq\; &-\theta(t)\varsigma_4\underline{\eta}x_2^2(t) + x_2(t)\delta_1(t) \\ &+ \theta(t)c_{\triangle}q_0^2\varsigma_4\overline{\eta}\int_{t-\tau}^{t}\int_{m-\tau}^{m} e^{q_0(\ell-t)}\int_{\mathcal{D}(\ell)}^{t}|x_2(t)\dot{x}_2(s)|\mathrm{d}s\mathrm{d}\ell\mathrm{d}m\end{aligned} \tag{58}$$

and so also

$$\begin{aligned}\dot{V}_0(t) \;&\leq\; -\theta(t)\varsigma_4\underline{\eta}x_2^2(t) + x_2(t)\delta_1(t) \\ &\quad + \theta(t)c_\triangle q_0^2\varsigma_4\overline{\eta}\int_{t-\tau}^{t}\int_{m-\tau}^{m} e^{q_0(\ell-t)}\int_{t-2\tau-\overline{\mathcal{D}}}^{t}|x_2(t)\dot{x}_2(s)|\mathrm{d}s\mathrm{d}\ell\mathrm{d}m \\ &\leq\; -\theta(t)\varsigma_4\underline{\eta}x_2^2(t) + x_2(t)\delta_1(t) + \theta(t)\varsigma_4\overline{\eta}\int_{t-2\tau-\overline{\mathcal{D}}}^{t}|x_2(t)\dot{x}_2(s)|\mathrm{d}s\ .\end{aligned} \tag{59}$$

By using the bound

$$|x_2(t)\dot{x}_2(s)| \leq \tfrac{\underline{\eta}}{2(2\tau+\overline{\mathcal{D}})\overline{\eta}}x_2^2(t) + \tfrac{(2\tau+\overline{\mathcal{D}})\overline{\eta}}{2\underline{\eta}}\dot{x}_2^2(s) \tag{60}$$

to upper bound the last integrand in (59), then our choice $c_* = \varsigma_1\varsigma_3\overline{\eta}^2(2\tau+\bar{\mathcal{D}})/(2\underline{\eta})$ gives

$$\begin{aligned}\dot{V}_0(t) \;&\leq -\theta(t)\varsigma_4\underline{\eta}x_2^2(t) + \theta(t)\varsigma_4\overline{\eta}\int_{t-2\tau-\overline{\mathcal{D}}}^{t}\Big(\tfrac{\underline{\eta}}{2(2\tau+\overline{\mathcal{D}})\overline{\eta}}x_2^2(t) + \tfrac{(2\tau+\overline{\mathcal{D}})\overline{\eta}}{2\underline{\eta}}\dot{x}_2^2(s)\Big)\mathrm{d}s + x_2(t)\delta_1(t) \\ &\leq -\tfrac{1}{2}\theta(t)\varsigma_4\underline{\eta}x_2^2(t) + \Big\{c_*\int_{t-2\tau-\overline{\mathcal{D}}}^{t}\dot{x}_2^2(s)\mathrm{d}s\Big\} + x_2(t)\delta_1(t).\end{aligned} \tag{61}$$

Let

$$W_1(x_{2,t}) = V_0(x_2(t)) + c_*(1+\epsilon)\int_{t-2\tau-\overline{\mathcal{D}}}^{t}\int_a^t \dot{x}_2^2(s)\mathrm{d}s\mathrm{d}a. \tag{62}$$

Then we can combine (56) and (61) to obtain

$$\begin{aligned}\dot{W}_1 &\leq -\tfrac{1}{2}\theta(t)\varsigma_4\underline{\eta}x_2^2(t) + c_*(1+\epsilon)(2\tau+\overline{\mathcal{D}})\dot{x}_2^2(t) + x_2(t)\delta_1(t) - \epsilon\mathcal{L}(t) \\ &= -\tfrac{1}{2}\theta(t)\varsigma_4\underline{\eta}x_2^2(t) + x_2(t)\delta_1(t) - \epsilon\mathcal{L}(t) \\ &\quad + c_*(1+\epsilon)(2\tau+\overline{\mathcal{D}})\left[\delta_1(t) - \theta(t)c_\triangle q_0^2\int_{t-\tau}^{t}\int_{m-\tau}^{m} e^{q_0(\ell-t)}\varsigma_4\eta(\ell)x_2(\mathcal{D}(\ell))\mathrm{d}\ell\mathrm{d}m\right]^2,\end{aligned} \tag{63}$$

where $\mathcal{L}(t)$ is the quantity in curly braces in (61), and where we used (31) with $\overline{\tau} = 2\tau + \overline{\mathcal{D}}$ and $\phi(s) = \dot{x}_2^2(s)$. If we use

$$x_2(t)\delta_1(t) \leq \tfrac{\epsilon}{2}\theta(t)\varsigma_4\underline{\eta}x_2^2(t) + \tfrac{\delta_1^2(t)}{2\epsilon\underline{\theta}\varsigma_4\underline{\eta}} \tag{64}$$

to upper bound the term $x_2(t)\delta_1(t)$ in (63) and then apply the relation $(a+b)^2 \leq (1+1/\epsilon)a^2 + (1+\epsilon)b^2$ to upper bound the quantity in square brackets in (63) and then apply Jensen's inequality to the squared integral that results, then we obtain

$$\begin{aligned}\dot{W}_1 &\leq -\tfrac{1-\epsilon}{2}\underline{\theta}\varsigma_4\underline{\eta}x_2^2(t) + \tfrac{1}{2\epsilon\underline{\theta}\varsigma_4\underline{\eta}}\delta_1^2(t) + c_{**}\int_{t-2\tau-\overline{\mathcal{D}}}^{t} e^{2q_0(\ell-t)}\varsigma_4^2\overline{\eta}^2x_2^2(\mathcal{D}(\ell))\mathrm{d}\ell \\ &\quad -\epsilon\mathcal{L}(t) + (1+1/\epsilon)c_*(1+\epsilon)\left(2\tau+\overline{\mathcal{D}}\right)\delta_1^2(t) \\ &\leq -\tfrac{1-\epsilon}{2}\underline{\theta}\varsigma_4\underline{\eta}x_2^2(t) + c_{**}\overline{\eta}^2\varsigma_4^2\int_{t-2\tau-2\overline{\mathcal{D}}}^{t}x_2^2(\ell)\mathrm{d}\ell - \epsilon\mathcal{L}(t) + 2c_*(1+\epsilon)(2\tau+\overline{\mathcal{D}})\delta_1^2(t) + \tfrac{\delta_1^2(t)}{2\epsilon\underline{\theta}\varsigma_4\underline{\eta}},\end{aligned}$$

where $c_{**} = c_\triangle^2 q_0^4 c_* \tau^2(1+\epsilon)^2(2\tau+\bar{\mathcal{D}})^2$ as before.

Therefore, since (32d) and our choices $\varsigma_4 = \varsigma_1\varsigma_3$ and $\underline{\theta} = \sqrt{2}/\pi$ imply that $2(\tau + \overline{\mathcal{D}})(1 + \epsilon)c_{**}\overline{\eta}^2\varsigma_4^2 < \frac{1-\epsilon}{2}\underline{\theta}\varsigma_4\underline{\eta}$, we can find positive constants w_* and w_{**} such that the time derivative of

$$W_2(x_{2t}) = W_1(x_{2t}) + (1+\epsilon)c_{**}\overline{\eta}^2\varsigma_4^2 \int_{t-2\tau-2\overline{\mathcal{D}}}^{t}\int_{\ell}^{t} x_2^2(p)\mathrm{d}p\mathrm{d}\ell \tag{65}$$

along all solutions of (48) satisfies $\dot{W}_2 \leq -w_* W_2(x_{2t}) + w_{**}\delta_1^2(t) - (\epsilon/2)\mathcal{L}(t)$, by applying (31) with $\overline{\tau} = 2(\tau + \overline{\mathcal{D}})$ and $\phi(s) = x_2^2(s)$. Also, if we let V_2 denote a quadratic global strict Lyapunov function for the uniformly globally exponentially stable system

$$\dot{z}_1(t) = q_0[-z_1(t) + z_2(t)], \quad \dot{z}_2(t) = -q_0 z_2(t), \tag{66}$$

then we can use $y_2(t) = \eta(t)x_2(\mathcal{D}(t))$ to find positive constants v_* and v_{**} such that

$$\dot{V}_2 \ \leq \ -v_* V_2(z(t)) + v_{**}\left[x_2^2(t) + \int_{t-\overline{\mathcal{D}}}^{t}\dot{x}_2^2(\ell)\mathrm{d}\ell\right] \tag{67}$$

along all solutions of the z subsystem in (14) with $z(0) = 0$. Since W_2 admits a positive definite quadratic lower bound in $x_2(t)$, and since the ω dynamics are uniformly globally exponentially stable to 0, we can then find positive constants $\bar{c}_i$ for $i = 1, 2, 3$ such that the time derivative of $V_4(x_{2t}, \omega(t), z(t)) = \bar{c}_1 W_2(x_{2t}) + \bar{c}_2 V_3(\omega(t)) + V_2(z(t))$ satisfies $\dot{V}_4 \leq -\bar{c}_3 V_4(x_{2t}, \omega(t), z(t))$ along all solutions of the (x_2, z, ω) dynamics for all $t \geq t_d(|(x_2(0), \omega(0))|) + 6\tau + 2\overline{\mathcal{D}}$ where V_3 is a positive definite quadratic Lyapunov function for the ω dynamics. This and the linear growth of the dynamics and our definitions of the ω_i's ensure that (25) is uniformly globally exponentially stable to 0, with an exponential decay rate that is independent of the function ϖ in (25) and therefore completes the proof of Theorem 3.

REFERENCES

[1] Bialy, B., Klotz, J., Curtis, J., and Dixon, W., "An Adaptive Backstepping Controller for a Hypersonic Air-Breathing Missile," *Proceedings of the AIAA Guidance Navigation and Control Conference*, AIAA, Reston, VA, August 2012, Paper AIAA2012-4468.
doi: 10.2514/6.2012-4468

[2] Chen, J., Dixon, W., Wagner, J., and Dawson, D., "Exponential Tracking Control of a Hydraulic Proportional Directional Valve and Cylinder via Integrator Backstepping," *Proceedings of the International Mechanical Engineering Congress and Exposition*, American Society of Mechanical Engineers, New York, NY, Nov. 2002, Paper IMECE2002-32076.
doi: 10.1115/IMECE2002-32076

[3] Sezkin, A., and Krstic, M., "Boundary Backstepping Control of Flow-Induced Vibrations of a Membrane at High Mach Numbers," *American Society of Mechanical Engineers Journal of Dynamic Systems, Measurement, and Control*, Vol. 137, No. 8, 2015, Paper DS-14-1203.
doi: 10.1115/1.4029468

[4] Zhu, Y., Krstic, M., Su, H., and Xu, C., "Linear Backstepping Output Feedback Control for Uncertain Linear Systems," *International Journal of Adaptive Control and Signal Processing*, Vol. 30, No. 8-10, 2016, pp. 1080–1098.
doi: 10.1002/acs.2542

[5] Mazenc, F., and Malisoff, M., "New Control Design for Bounded Backstepping under Input Delays," *Automatica*, Vol. 66, 2016, pp. 48–55.
doi: 10.1016/j.automatica.2015.12.012

[6] Mazenc, F., Malisoff, M., Burlion, L., and Weston, J., "Bounded Backstepping Control and Robustness Analysis for Time-Varying Systems under Converging-Input-Converging-State Conditions," *European Journal of Control*, Vol. 42, 2018, pp. 15–24.
doi: 10.1016/j.ejcon.2018.02.005

[7] Hu, T., "A Nonlinear-System Approach to Analysis and Design of Power-Electronic Converters with Saturation and Bilinear Terms," *Institute of Electrical and Electronics Engineers Transactions on Power Electronics*, Vol. 26, No. 2, 2011, pp. 399–410.
doi: 10.1109/TPEL.2010.2054115

[8] Hu, T., and Lin, Z., *Control Systems with Actuator Saturation*, Birkhauser, Boston, MA, 2001.

[9] Li, Y., and Lin, Z., *Stability and Performance of Control Systems with Actuator Saturation*, Birkhauser, Boston, MA, 2018.
doi: 10.1007/978-3-319-64246-8

[10] Palmeira, A., Gomes da Silva Jr., J., Tarbouriech, S., and Ghiggi, I., "Sampled-Data Control under Magnitude and Rate Saturating Actuators," *International Journal of Robust and Nonlinear Control*, Vol. 26, No. 15, 2016, pp. 3232–3252.
doi: 10.1002/rnc.3503

[11] Seuret, A., and Gomes da Silva Jr., J., "Taking into Account Period Variations and Actuator Saturation in Sampled-Data Systems," *Systems and Control Letters*, Vol. 61, No. 12, 2012, pp. 1286–1293.
doi: 10.1016/j.sysconle.2012.09.003.

[12] Tarbouriech, S., Garcia, G., Gomes da Silva Jr., J., and Queinnec, I., *Stability and Stabilization of Linear Systems with Saturating Actuators*, Springer-Verlag, Berlin, Germany, 2011.
doi: 10.1007/978-0-85729-941-3.

[13] Tarbouriech, S., and Gomes da Silva Jr, J., "Synthesis of Controllers for Continuous-Time Delay Systems with Saturating Controls via LMIs," *Institute of Electrical and Electronics Engineers Transactions on Automatic Control*, Vol. 45, No. 1, 2000, pp. 105–111.
doi: 10.1109/9.827364

[14] Karagiannis, D., and Astolfi, A., "A New Solution to the Problem of Range Identification in Perspective Vision Systems," *Institute of Electrical and Electronics Engineers Transactions on Automatic Control*, Vol. 50, No. 12, 2005, pp. 2074–2077.
doi: 10.1109/TAC.2005.860269

[15] Le Bras, F., Hamel, T., Mahony, R., Barat, C., and Thadasack, J., "Approach Maneuvers for Autonomous Landing using

Visual Servo Control," *Institute of Electrical and Electronics Engineers Transactions on Aerospace and Electronic Systems*, Vol. 50, No. 2, 2014, pp. 1051–1065.
doi: 10.1109/TAES.2013.110780

[16] Serra, P., Cunha, R., Hamel, T., Cabecinhas, D., and Silvestre, C., "Landing of a Quadrotor on a Moving Target using Dynamic Image-Based Visual Servo Control," *Institute of Electrical and Electronics Engineers Transactions on Robotics*, Vol. 32, No. 6, 2016, pp. 1524–1535.
doi: 10.1109/TRO.2016.2604495

[17] Bourquardez, O., and Chaumette, F., "Visual Servoing of an Airplane for Auto-Landing," *Proceedings of the 2007 International Conference on Intelligent Robots and Systems*, Institute of Electrical and Electronics Engineers, Piscataway, NJ, Nov. 2007, pp. 1314–1319.
doi: 10.1109/IROS.2007.4399216

[18] Coutard, L., Chaumette, F., and Pflimlin, J., "Automatic Landing on Aircraft Carrier by Visual Servoing," *Proceedings of the International Conference on Intelligent Robots and Systems*, Institute of Electrical and Electronics Engineers, Piscataway, NJ, Sept. 2011, pp. 2843–2848.
doi: 10.1109/IROS.2011.6094887

[19] Burlion, L., and de Plinval, H., "Vision Based Anti-Windup Design with Application to the Landing of an Airliner," *Proceedings of the 20th World Congress*, International Federation of Automatic Control, New York, NY, July 2017, pp. 10482–10487.
doi: 10.1016/j.ifacol.2017.08.1978

[20] Mazenc, F., Burlion, L., and Malisoff, M., "Stabilization and Robustness Analysis for a Chain of Saturating Integrators with Imprecise Measurements," *Institute of Electrical and Electronics Engineers Control Systems Letters*, Vol. 3, No. 2, 2019, pp. 428–433.
doi: 10.1109/LCSYS.2019.2892931

[21] Mazenc, F., Burlion, L., and Gibert, V., "Stabilization of a Nonlinear System that Arises in the Context of Vision Based Landing of an Airliner," *Proceedings of the Conference on Decision and Control*, Institute of Electrical and Electronics Engineers, Piscataway, NJ, December 2018, pp. 5313–5318.
doi: 10.1109/CDC.2018.8619686

[22] Khalil, H., *Nonlinear Systems, Third Edition*, Prentice Hall, Upper Saddle River, NJ, 2002.

[23] Sepulchre, R., Jankovic, M., and Kokotovic, P., *Constructive Nonlinear Control*, Springer-Verlag, Berlin, Germany, 1996.

[24] Burlion, L., and de Plinval, H., "Toward Vision Based Landing of a Fixed-Wing UAV on an Unknown Runway under Some FOV Constraints," *Proceedings of the International Conference on Unmanned Aircraft Systems*, Institute of Electrical and Electronics Engineers, Piscataway, NJ, June 2017, pp. 1824–1832.
doi: 10.1109/ICUAS.2017.7991333